Desalination and Water Treatment
www.deswater.com
doi: 10.1080/19443994.2015.1031710

57 (2016) 9824–9836
May

Taylor & Francis
Taylor & Francis Group

Design analysis of fixed-bed synergic adsorption of heavy metals and acid blue 25 on activated carbon

M.T. Hernandez-Eudave, A. Bonilla-Petriciolet*, M.R. Moreno-Virgen, C.K. Rojas-Mayorga, R. Tovar-Gómez

Chemical Engineering Department, Instituto Tecnológico de Aguascalientes, C.P. 20256 Aguascalientes, México, Tel. +52 4499105002; emails: theudave@yahoo.com.mx (M.T. Hernandez-Eudave), petriciolet@hotmail.com (A. Bonilla-Petriciolet), rosario-moreno2011@hotmail.com (M.R. Moreno-Virgen), karymayorga@yahoo.com.mx (C.K. Rojas-Mayorga), rigtogo@hotmail.com (R. Tovar-Gómez)

Received 7 December 2014; Accepted 13 March 2015

ABSTRACT

This study reports the multicomponent adsorption of dye AB25, nickel (Ni^{2+}) and zinc (Zn^{2+}) ions on an activated carbon using binary mixtures of metal and dye, and packed bed columns at different operating conditions. Design parameters of packed bed adsorption columns have been calculated using the breakthrough curves and Thomas model, and an analysis has been performed to determine the effect and magnitude of the synergistic adsorption on the design parameters and adsorbent performance. Results showed that there is a strong synergistic adsorption of heavy metals on activated carbon caused by the presence of dye AB25 in binary mixtures. The magnitude of this synergistic adsorption effect depends on the dynamic operating conditions and type of heavy metal present in the binary system. The presence of dye AB25 in the binary mixtures caused a better degree of column utilization because the values of mass transfer zone decreased with respect to the results obtained with mono-component solutions. Metal adsorption capacities may increase up to 20 times if the binary mixture with dye AB25 is used as a column feed. In addition, the removal of heavy metal ions in adsorption columns packed with dye-loaded activated carbon is also an effective treatment process. This improvement in metal adsorption capacities is due to dye AB25 loaded in activated carbon may act as an additional active site for binding the metallic ions. In summary, this study showed that an adsorbent with a lower adsorption capacity for the removal of heavy metals can be employed, without comprising the process efficacy, in the treatment of multicomponent mixtures of dyes and heavy metals under dynamic operating conditions.

Keywords: Packed bed columns; Multicomponent adsorption; Dyes; Heavy metals; Activated carbon

1. Introduction

Adsorption process is an effective method for purification of water and wastewaters polluted by a wide variety of organic and inorganic toxic compounds. This separation process offers both economic and technical advantages in comparison to other available water treatment technologies. To date, the activated carbon is still the universal adsorbent used for water purification because it can be synthesized from

*Corresponding author.

a wide variety of low-cost precursors and its adsorption properties can be tailored to remove a specific pollutant [1–3].

Overall, the literature on adsorption process using activated carbons is mainly related to mono-component solutions (i.e. solutions with only one pollutant). In these studies, the removal performance of the activated carbon is tested using solutions with one adsorbate at different operating conditions (i.e. pH, temperature, pollutant concentration, adsorbent dosage). This type of experiments provides results that correspond to an ideal behavior of the adsorbent because real-life fluids may contain different dissolved pollutants (i.e. they are multicomponent systems). The presence of several pollutants in the same solution may significantly affect the removal performance of the adsorbent causing increments or decrements of the adsorption capacities, depending on the characteristics of the multicomponent solution [4–6]. For this scenario, the adsorbent performance depends on the quantity, type, and concentration of the pollutants present in the multicomponent solution. Therefore, the study of multicomponent adsorption process is relevant for the process design of water and wastewater treatment strategies.

In particular, the activated carbon is an effective adsorbent for the removal of both heavy metals and dyes from aqueous solution [1,7,8]. There is a vast amount of literature related to the adsorption of both heavy metals and dyes in batch adsorption systems using activated carbon and mono-component solutions [9–13]. Herein, it is convenient to remark that batch adsorption studies are useful to determine relevant thermodynamic and kinetic parameters of the removal process, e.g. maximum adsorption capacities and adsorption rates. On the other hand, recent studies have reported the simultaneous adsorption of dyes and heavy metals on activated carbon and other adsorbents using binary systems at batch operating conditions, e.g. [14–21]. This type of multicomponent solutions (i.e. mixtures of dyes and heavy metals) can be found in real-life conditions because several industries may generate effluents where both toxic pollutants can co-exist [18,21]. Multicomponent adsorption studies of dyes and heavy metals using different adsorbents (e.g. zeolites, graphene oxide, fly ash, polymers, composites) at batch conditions have concluded that dyes may cause both antagonistic and synergistic adsorption effects in the removal of heavy metal ions, where the magnitude and type of these effects depend on the physicochemical properties of the dye and adsorbent under study. For example, Tovar-Gómez et al. [16] and Aguayo-Villarreal et al. [17] have reported that dye AB25 enhanced the adsorption of heavy metal ions on activated carbons in binary mixtures of dye and heavy metal; while Visa et al. [14] have concluded that methylene blue competed with heavy metal ions during the multicomponent adsorption on fly ash. So, the analysis of multicomponent adsorption of these mixtures is fundamental to perform the proper design of reliable water purification technologies for real-life applications.

Dynamic adsorption systems based on packed bed columns are commonly employed in industrial applications and this configuration system is easy to use and useful to perform lab experiments for establishing design parameters [22–24]. These adsorption systems allow to determine the maximum performance of the adsorbent and to identify the best dynamic operating conditions. However, to the best of the author's knowledge, there is a lack of studies on the simultaneous adsorption of heavy metals and dyes on activated carbon using packed bed columns. These studies are important to determine if the antagonistic and synergistic adsorption effects observed in batch studies for the mixtures of dye and metal ion can occur and to establish their magnitude under the mass transfer conditions of the dynamic adsorption process. Herein, it is important to remark that the operating conditions of dynamic adsorption systems imply residence times lower than the equilibrium time and there are also mass transfer resistances. Therefore, the results of dynamic adsorption studies can be used for establishing the feasibility of taking advantage of the synergic adsorption effects, or controlling the negative impacts of antagonistic adsorption, involved in the simultaneous removal of metals and dye using real-life operating conditions.

This study reports the multicomponent adsorption of dye AB25, nickel (Ni^{2+}) and zinc (Zn^{2+}) ions on a commercial activated carbon using binary mixtures of metal and dye, and packed bed columns. In particular, the simultaneous adsorption of these pollutants has been analyzed at different operating conditions of the packed bed columns. Design parameters of packed bed adsorption columns have been calculated using the breakthrough curves and Thomas model, and an analysis has been performed to determine the effect and magnitude of the synergistic adsorption on the design parameters and adsorbent performance. Finally, the experimental data have been employed to understand the possible interactions and removal mechanism involved in the simultaneous removal of both types of pollutants using activated carbon.

2. Methodology

2.1. Activated carbon and its physicochemical characterization

Adsorption studies were performed using a commercial activated carbon, which has been purchased from Clarimex Company (Mexico). Table 1 shows the main physicochemical properties of this low-cost commercial adsorbent including its elemental composition and textural parameters. This commercial adsorbent has a significant BET surface area (~941 m^2/g) and an apparent density of ~0.4 g/mL; however, preliminary studies indicated that its adsorption properties for the removal of heavy metal ions Ni^{2+} and Zn^{2+} are lower than 1.0 mg/g at 308.15 K (i.e. 35˚C) and pH 5. Therefore, this adsorbent has been selected as case of study to characterize and quantify the synergic adsorption effects caused by dye AB25 on the simultaneous removal of binary systems of dye and heavy metal using packed bed adsorption columns. This adsorbent was washed with deionized water and sieved to obtain a mean particle diameter of 1 mm, which was used for the dynamic adsorption experiments.

Different characterization techniques were used to study the surface chemistry of the activated carbon before and after its application in adsorption experiments. Specifically, the functional groups of activated carbon were determined using transmission FT-IR spectra recorded on a Bruker IFS 66/S spectrophotometer. Adsorbent samples were analyzed together with spectroscopic grade KBr, where a resolution of $4\ cm^{-1}$ and 200 scans were used. The chemical composition of the activated carbon surface was analyzed using X-ray photoelectron spectroscopy (XPS). This analysis was performed with a Prevac photoelectron spectrometer equipped with a hemispherical analyzer (VG SCIENTA R3000). Spectra were taken using a mono-chromatized aluminum source Al Kα (E = 1486.6 eV). The base pressure in the analytical chamber was 5×10^{-9} mbar. The binding energy scale was calibrated using the Au 4f7/2 line of a cleaned gold sample at 84.0 eV. Results from these characterization techniques were employed to establish the possible adsorption mechanism involved in the multicomponent adsorption of heavy metals and dye AB25 on tested adsorbent.

Table 1
Physicochemical properties of the commercial activated carbon used in this study

Elemental composition	%	Physicochemical property	
Carbon	72.2	Acidity (mmol/g)	2.71
Hydrogen	3.3	Basicity (mmol/g)	0.17
Nitrogen	1.4	S_{BET} (m^2/g)	941
Sulfur	0.2	V_{total} (cm^3/g)	0.9124
Oxygen	22.9	D_p (nm)	2.8

2.2. Dynamic adsorption experiments using packed bed columns and binary solutions of dye AB25 and heavy metals

Dynamic adsorption experiments were performed using a glass column of 17 cm of height and 2.5 cm of internal diameter. A sample of 9.35 g of activated carbon was used in all adsorption experiments. Packed bed adsorption columns were operated at 308.15 K (i.e. 35˚C), pH 5 of feed solution, and using a feed flow rate of 3.2 mL/min (i.e. a residence time of ≈3 min). Note that the operating conditions for pH, temperature, and feed flow rate were selected to obtain the best adsorption performance of activated carbon. Different adsorption studies were performed in packed bed columns using the following operating conditions: (1) Breakthrough curves of mono-component solutions of both dye AB25 and heavy metals Ni^{2+} and Zn^{2+} using raw activated carbon; (2) Breakthrough curves of binary solutions of AB25 + Ni^{2+} and AB25 + Zn^{2+} using raw activated carbon; and (3) Breakthrough curves of mono-component solutions of heavy metals Ni^{2+} and Zn^{2+} but using activated carbon loaded with dye AB25. Note that Ni^{2+} and Zn^{2+} were selected in this study because these ions are commonly present in the wastewater of several industries and they are considered as toxic heavy metals. Adsorption experiments using mono-component solutions were used as a comparative basis in the data analysis for identifying the presence and magnitude of synergistic adsorption effects on the simultaneous removal of AB25 and heavy metal ions. All dynamic adsorption experiments were performed using a feed concentration of 400 mg/L for dye AB25, and 20 and 30 mg/L for both Ni^{2+} and Zn^{2+} ions.

The performance and efficacy of the packed bed adsorption columns were determined via the analysis of breakthrough curves. Several samples of the adsorption column outlet were obtained for determining the pollutants concentrations, which were used for determining the profile $[Pollutant]_{outlet}/[Pollutant]_{inlet}$ vs. the operating time of packed bed adsorption column. All adsorption columns were operated until the outlet concentration of the column $[Pollutant]_{outlet}$ was 95% of the feed concentration $[Pollutant]_{inlet}$. This operating point was considered as the saturation condition of the adsorbent.

For the case of dynamic adsorption experiments using the dye-loaded activated carbon, first, the raw

activated carbon was used in the packed bed column for the adsorption of AB25 dye employing a feed solution of 400 mg/L. Later, a feed solution with the heavy metal under analysis (i.e. Ni^{2+} or Zn^{2+}) was introduced to the same column, which was packed with the dye-loaded activated carbon. This column was operated until reaching the saturation point of the adsorbent (i.e. 95% of the feed concentration). These experiments were performed to identify the possible interactions between metal ions and dye AB25 during the multicomponent dynamic adsorption process using activated carbon. In all experiments, the heavy metal concentrations were determined using atomic absorption spectroscopy while UV–vis spectrometry at 600 nm was used for the dye quantification. All experiments were performed by duplicate and the mean values were used for data analysis.

2.3. Design analysis of packed bed adsorption columns

Results of breakthrough curves of both mono-component and binary solutions were used for the calculation of design parameters of packed bed adsorption columns. Specifically, the mass transfer zone (MTZ) was estimated for all breakthrough curves using the next equation:

$$\mathrm{MTZ} = L\left(\frac{t_e - t_b}{t_e}\right) \tag{1}$$

where L is the bed height in cm, t_e and t_b are the saturation and breakthrough times obtained from the breakthrough curve given in h, respectively. For data analysis of adsorption columns, t_b was defined as the operation time of breakthrough curve where $[\mathrm{Pollutant}]_{outlet}/[\mathrm{Pollutant}]_{inlet} = 0.05$, while t_e corresponds to $[\mathrm{Pollutant}]_{outlet}/[\mathrm{Pollutant}]_{inlet} = 0.95$, respectively. These values are commonly used for breakthrough analysis in water treatment [24,25]. The overall adsorption zone (Δt) was also calculated to determine the performance of activated carbon in dynamic removal experiments. This parameter is given by:

$$\Delta t = t_e - t_b \tag{2}$$

which is also given in h.

Retardation factors (r_f) of all adsorption columns were used to determine the rate at which the pollutant moved within the packed bed columns [26]. These factors have been obtained from the treated volume per void volume that gives $[\mathrm{Pollutant}]_{outlet}/[\mathrm{Pollutant}]_{inlet} = 0.5$ or, equivalently, the operating time ($t_{50\%}$) of the packed bed adsorption column when the effluent concentration has reached 50% of the influent concentration. So, r_f is defined as:

$$r_f = \frac{V_{50\%}}{AL\,\varepsilon} \tag{3}$$

where ε is the column void fraction of the packed bed column (~0.3), A is the cross-sectional area of the column reported in cm^2, and L is the bed height of the column given in cm, respectively. Retardation factors were estimated for all operating conditions used in the dynamic adsorption experiments.

The bed adsorption capacities (q_{bed}) were calculated using the Thomas breakthrough equation [27]. This breakthrough model is based on Langmuir-type adsorption–desorption and assumes isothermal and isobaric operating conditions, a constant column void fraction, and the radial and axial dispersion are negligible in the packed bed column [27]. In particular, this model is given by:

$$\frac{[A]_t}{[A]_0} = \frac{1}{1 + \exp\left(\frac{k_{Th}}{Q}\left(q_{bed,T}W_{bed} - [A]_0 V_{eff}\right)\right)} \tag{4}$$

where $[A]_t$ is the concentration (mg/L) of pollutant A in the column outlet at time t, $[A]_0$ is the concentration (mg/L) of pollutant A in the feed, V_{eff} is the treated volume of the mono-component or binary solution in L, Q is the feed flow rate in L/h, W_{bed} is the amount of activated carbon packed in the column and is given in g, $q_{bed,T}$ is the adsorption capacity of the packed bed column estimated by the model given and is given in mg/g, and k_{Th} is the Thomas rate constant reported in L/h mg. Parameters k_{Th} and $q_{bed,T}$ were obtained from a non-linear regression approach using the simulated annealing method [28].

All design parameters were used for characterizing the performance of the activated carbon in adsorption columns employing both mono-component and binary solutions. In particular, a dimensionless performance ratio has been used for the analysis of design parameters of packed bed adsorption columns

$$R_D = \frac{D_{mix}}{D_0} \tag{5}$$

where D_{mix} is the design parameter calculated from the breakthrough curve using the binary solutions of dye and metal ion, D_0 is the same design parameter but calculated using the breakthrough curve with the mono-component solution at the same operating

conditions of the binary solution, respectively. The values of R_D are used to identify the presence of synergistic adsorption effects and their impact on the performance of packed bed adsorption columns using the binary solutions. Note that it is expected that the values of $R_D > 1.0$ for several design parameters of breakthrough curves of the metal ion in the binary mixture. This is because the adsorbent performance for the removal of the metal ion may be enhanced by the presence of the dye AB25. This trend is expected to apply for t_b, t_e, r_f, Δt, and q_{bed}.

3. Results and discussion

3.1. Breakthrough curves for the simultaneous adsorption of dye AB25 and heavy metals

Fig. 1 shows the breakthrough curves of the adsorption of dye AB25, Ni^{2+} and Zn^{2+} on the activated carbon using the mono-component feed solutions. Table 2 provides the design parameters calculated from these breakthrough curves for tested pollutants including the results of breakthrough data modeling with Thomas equation. As stated, these results are the basis for the comparison and analysis of breakthrough curves of binary mixtures of dye and metal ion. All mono-component breakthrough curves show the traditional S-shape where their characteristics depend on the pollutant type and concentration. It is convenient to note that breakthrough curves showed the common characteristic of adsorption processes in a liquid phase that implies a slow approach of $[Pollutant]_{outlet}/[Pollutant]_{inlet} \rightarrow 1.0$, which is associated to the fact that the diffusion phenomenon is the rate-limiting mass transport process.

The service time of dye breakthrough curve is higher than those obtained for both Zn^{2+} and Ni^{2+} ions. On the other hand, the breakthrough curves for the heavy metals indicated that the operation time is higher for Zn^{2+} than that obtained for Ni^{2+}. Also, it is clear that the operation time decreased with the feed concentration for both metal ions, see Fig. 1 and Table 2. Both t_b and t_e are different for both dye and metal ions depending on the operating conditions of the packed bed adsorption columns. For heavy metals, Table 2 indicates that the value of MTZ increased with the feed concentration while the Thomas rate constants decreased with feed concentration. These results confirmed that the saturation of packed bed adsorption columns is faster if the feed concentration is also higher. Overall, when the feed concentration increased, the treated volume required to reach the exhaustion point is reduced. Breakthrough curves of metal ions showed this trend but the feed concentration has a minor impact on the adsorbent performance. According to the authors experience in dynamic adsorption systems [24,25], the effect of feed concentration on the performance of breakthrough curves of tested heavy metals is less significant than those obtained for other dynamic adsorption systems (i.e. pollutant + adsorbent). Probably, the effect observed in these experiments is due to the activated carbon used in the adsorption columns has a low metal adsorption capacity and the concentration

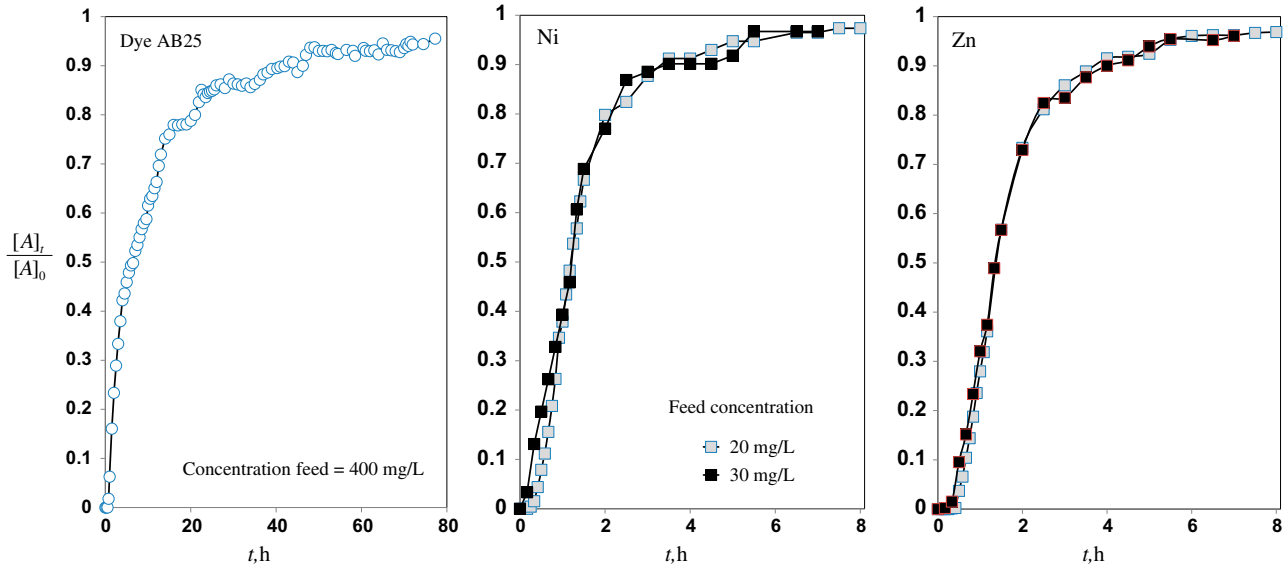

Fig. 1. Mono-component breakthrough curves for the adsorption of dye AB25, Ni^{2+} and Zn^{2+} on a commercial activated carbon at 308.15 K (i.e. 35°C) and pH 5.

Table 2
Design parameters of packed bed columns obtained from the mono-component breakthrough curves for the adsorption of heavy metal ions and dye AB25 on a commercial activated carbon

		Design parameters of packed bed columns					Thomas model		
Pollutant	$[Pollutant]_0$ (mg/L)	t_b (h)	t_e (h)	Δt (h)	MTZ (cm)	r_f	K_{Th} (L/h mg)	q_{bed} (mg/g)	R^2
Dye AB25	400	0.93	75.96	75.03	7.41	325.55	0.0038	66.97	0.89
Ni^{2+}	20	0.43	5.65	5.22	6.93	51.13	0.1286	0.53	0.97
	30	0.23	5.32	5.09	7.18	43.59	0.0721	0.67	0.98
Zn^{2+}	20	0.56	5.44	4.88	6.73	58.77	0.1152	0.60	0.99
	30	0.40	5.35	4.95	6.94	59.03	0.0615	0.91	0.97

gradients in the column do not cause a significant effect on the adsorbent performance at tested operating conditions. Mono-component adsorption capacities of activated carbon was 67 mg/g for dye AB25 and 0.53–0.67 mg/g for Ni^{2+}, and 0.60–0.91 mg/g for Zn^{2+}, see results reported in Table 2. These results indicate that the adsorption capacity of tested activated carbon is lower than 1.0 mg/g for these metal ions (i.e. it is not proper for heavy metal removal in mono-metallic solutions) while this adsorbent showed an acceptable performance for the removal of dye AB25 in mono-component solutions.

Fig. 2 shows the breakthrough curves for the adsorption of dye AB25 using the binary solutions as the column inlet. These results showed that the presence and concentration of heavy metal ions in the binary solution do not affect the adsorption of dye AB25 on activated carbon. In fact, the breakthrough curves for the adsorption of dye AB25 in both mono-component and binary solutions are equal. These findings confirmed the results obtained by Tovar-Gómez et al. [16] and Aguayo-Villarreal et al. [17] in batch adsorption systems using different activated carbons and binary solutions of metal and dye AB25, where there is no interaction on the adsorption of dye AB25 caused by the presence of heavy metal ions.

On the other hand, the breakthrough curves for the adsorption of Ni^{2+} and Zn^{2+} in binary mixtures are reported in Fig. 3. It is clear that the operation time and characteristics of these breakthrough curves vary significantly depending on the operating conditions. In contrast to the results obtained with the mono-metallic solutions, the effect of feed concentration of tested heavy metals on the characteristics of breakthrough curves using binary systems is evident, see Fig. 3.

3.2. Analysis of design parameters of breakthrough curves

Design parameters of packed bed adsorption columns obtained for heavy metal ions in binary solutions are reported in Table 3. These results

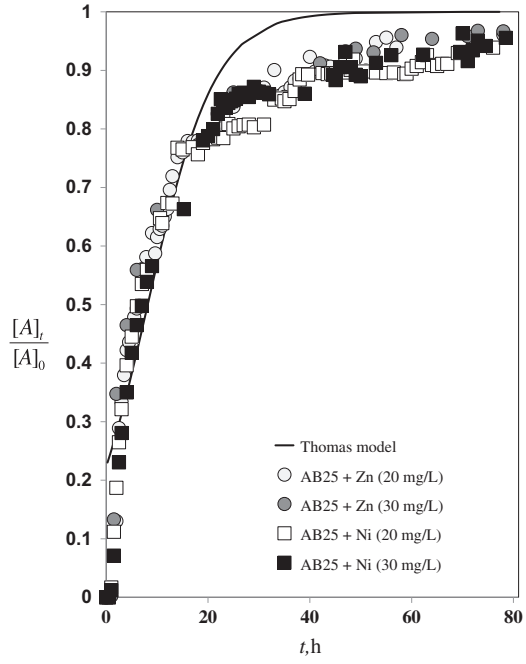

Fig. 2. Multicomponent breakthrough curves for the adsorption of dye AB25 on a commercial activated carbon using binary solutions of dye and metal at 308.15 K (i.e. 35°C) and pH 5.

showed that there is a great variation in the adsorbent performance in packed bed columns for the binary solution with respect to the results obtained for the mono-component systems. For example, the breakthrough and exhaustion times of breakthrough curves for both heavy metals using binary solutions vary significantly. For Ni^{2+} adsorption, t_b ranged from 9.06 to 12.4 h, while t_e ranged from 64.5 to 75.85 h for tested metal feed concentrations in binary solution (i.e. 20 and 30 mg/L). These operating times for Zn^{2+} are t_b: 17.05 and 23.88 h and t_e: 86.2 and 117.13 h, respectively. For low feed concentration of metal ions, the values of both t_b and t_e increased. Note that similar trends are identified for MTZ and r_f.

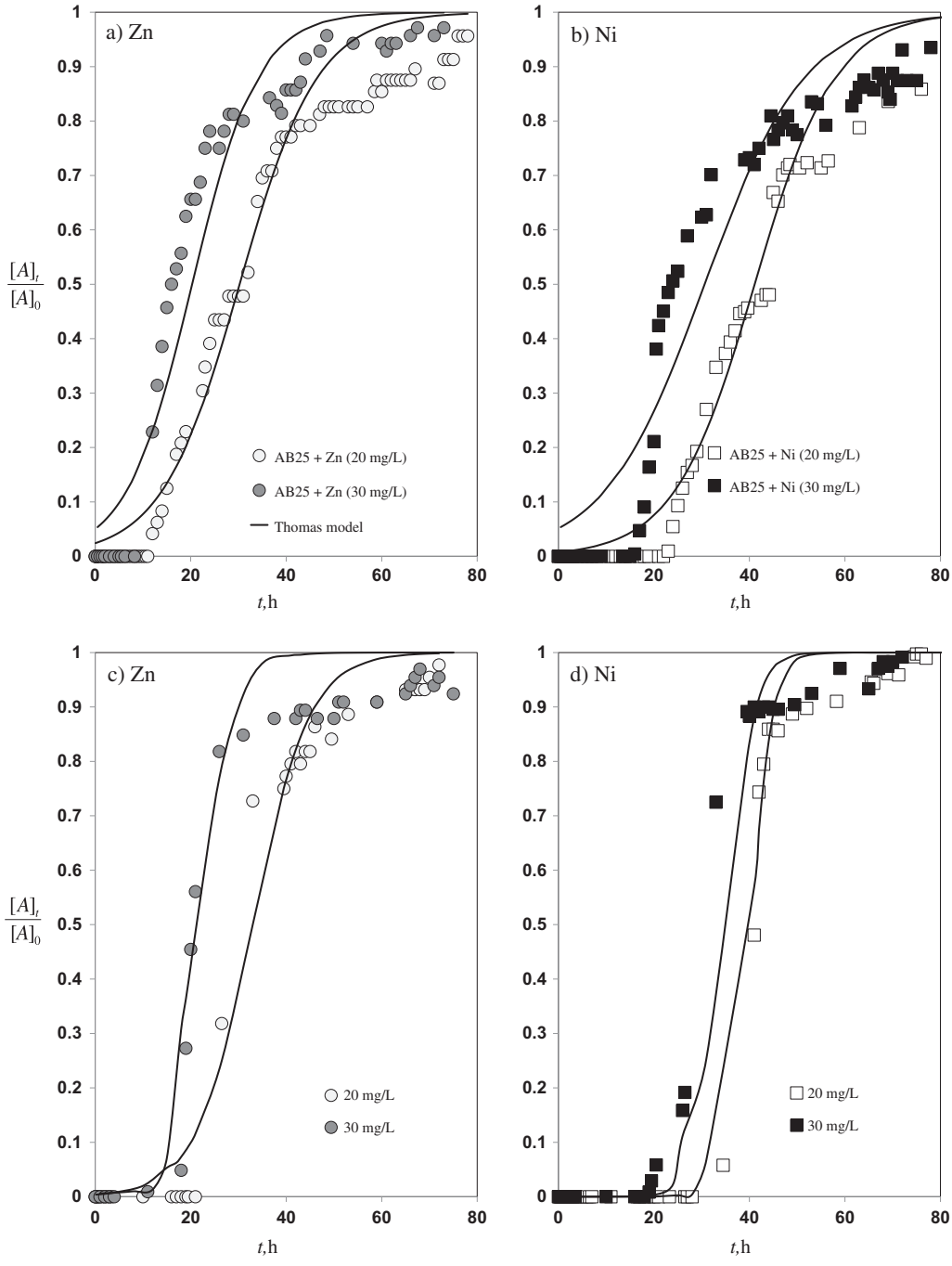

Fig. 3. Multicomponent breakthrough curves for the adsorption of heavy metals on a commercial activated carbon using binary solutions of dye and metal at 308.15 K (i.e. 35˚C) and pH 5. (a,b) Raw activated carbon and (c,d) dye-loaded activated carbon.

Table 4 shows the calculated values of R_D for the different design parameters obtained from the breakthrough curves. Overall, these results indicated that there was a significant increment on the adsorption of both Ni^{2+} and Zn^{2+} ions in binary solution feeds in comparison to the results obtained with the mono-component solutions. In general, the values of design parameters t_b, t_e, r_f, Δt, and q_{bed} for metal adsorption from binary solutions increased in one order of magnitude with respect to the results obtained for mono-component breakthrough curves. The increment in these parameters ranged from 1,100 to 6,000%,

Table 3
Design parameters of packed bed columns obtained from the binary breakthrough curves for the simultaneous adsorption of heavy metal ions and dye AB25 on a commercial activated carbon

			Design parameters of packed bed columns					Thomas model		
Mixture	Pollutant	Feed concentration (mg/L)	t_b (h)	t_e (h)	Δt (h)	MTZ (cm)	r_f	K_{Th} (L/h mg)	q_{bed} (mg/g)	R^2
AB25–Ni^{2+}	Ni^{2+}	400–20	9.06	64.5	55.44	6.45	1,240.34	0.0058	13.08	0.97
		400–30	12.4	75.85	63.45	6.27	736.30	0.0045	13.26	0.94
AB25–Zn^{2+}	Zn^{2+}	400–20	17.05	86.2	69.15	6.02	1,535.94	0.0062	16.03	0.97
		400–30	23.88	117.13	93.25	5.97	1,170.72	0.0031	18.86	0.92

Table 4
Performance ratios of the design parameters of packed bed columns used in the simultaneous adsorption of heavy metal ions and dye AB25 on a commercial activated carbon

			R_D for design parameters of packed bed adsorption columns						
Mixture	Pollutant	Feed concentration (mg/L)	t_b	t_e	Δt	MTZ	r_f	K_{Th}	q_{bed}
AB25–Ni^{2+}	Ni^{2+}	400–20	21.07	11.42	10.62	0.93	24.26	0.05	24.68
		400–30	53.91	14.26	12.47	0.87	16.89	0.06	19.79
AB25–Zn^{2+}	Zn^{2+}	400–20	30.45	15.85	14.17	0.89	26.13	0.05	26.72
		400–30	59.70	21.89	18.84	0.86	19.83	0.05	20.73

depending on the operating conditions and tested heavy metal. It is convenient to note that the effect of synergistic adsorption caused by AB25 was more significant for low concentrations of tested heavy metal ions especially for Zn^{2+}. The Thomas rate constants of heavy metals in binary systems significantly decreased with respect to the results obtained in mono-component breakthrough curves; see Table 4. Retardation factors r_f for heavy metal ions in binary breakthrough curves increased indicating that these pollutants are adsorbed more effectively in binary mixtures of dye and metal. Note that heavy metal ions will move faster inside the packed bed adsorption column with lower r_f than those columns with higher r_f. On the other hand, the calculated values of MTZ of binary breakthrough curves were lower, up to ≈ 15%, than those values obtained for mono-component breakthrough curves. The minimization of the length of MTZ implies that more of the adsorption capacity of the adsorbent is used for the removal process. Values of MTZ depend on the type of adsorbent used, the residence time, and the initial concentration of the pollutant in the column feed. This result confirmed that the heavy metal removal was more effective using binary mixtures of dye and metal and that the degree of column utilization increased because more of the bed of activated carbon was used in heavy metal adsorption.

In particular, the adsorption capacity of heavy metals on activated carbon increased up to 20 times using the binary mixtures. The estimated values of q_{bed} ranged from 24.7 to 19.8 mg/g for Ni^{2+} and from 26.7 to 20.7 for Zn^{2+}, respectively. These adsorption capacities are competitive with respect to those reported for other adsorbents in packed bed adsorption columns [23,29]. For example, the adsorption capacities obtained in binary mixtures of dye and metal are higher than those reported for activated carbon from Hevea brasiliensis: 20–30 mg/g for Ni^{2+} and 10–15 mg/g for Zn^{2+} [29] and palm shell activated carbon: 6–16 mg/g for Ni^{2+} [23]. Even though, the adsorbent used in this study showed a poor adsorption capacity of heavy metals using mono-component solutions, the presence of dye AB25 in the binary solution improved its removal performance. In fact, these results highlight the relevance of analyzing the adsorption performance in multicomponent systems in order to optimize and to design properly water treatment systems.

These findings confirmed that there was a strong synergistic effect for the adsorption of heavy metal ions on activated carbon caused by the presence of

dye AB25. In fact, the conclusion is that the synergistic adsorption effect observed in previous studies using batch conditions prevails for dynamic operating conditions. This result is very relevant from a practical point of view because, as stated, the dynamic adsorption systems may show some operational disadvantages due to the limitation in the contact time between adsorbent and fluid to be treated, and the presence of several resistances for mass transfer caused by the configuration of packed bed columns. So, the interaction metal ion-dye adsorbent is favorable in binary systems and helps to overcome some of these mass transfer resistances for the dynamic adsorption of heavy metals. In addition, it can be concluded that if a specific adsorbent does not show a significant adsorption capacity for the removal of heavy metal ions in mono-component solutions, it could be effectively used for the removal of metallic ions if the feed solution to be treated contains a dye that can promote a synergistic adsorption effect.

Fig. 3(c) and (d) show the breakthrough curves for the adsorption of heavy metal ions on dye-loaded activated carbon and Table 5 contains the design parameters for these curves. Overall, the design parameters of these breakthrough curves are different from those results obtained with the binary solutions. Note that breakthrough curves obtained with dye-loaded adsorbent are steeper than those obtained with the raw activated carbon and binary systems. The parameters t_b, t_e, and q_{bed} showed the most significant changes with respect to the results obtained for binary systems. Bed adsorption capacities of heavy metals on dye-loaded activated carbon are slightly higher (from 3 to 15%) than those values obtained in binary breakthrough curves, see Table 5. Also, the values of MTZ decreased in the experiments performed with dye-loaded adsorbent, indicating a better removal efficacy of adsorption columns under this operating mode. In fact, these results showed that an adsorbent with a low metal adsorption capacity can be used, first, in the removal of dye AB25 and, later, for the effective adsorption of heavy metal ions without compromising the performance of adsorption process. This context allows the independent treatment of fluids polluted with different compounds (i.e. dyes and heavy metals) by reusing the same adsorbent. It is convenient to note that Shukla and Pai [30] reported the adsorption of Ni^{2+} and Zn^{2+} on dye-loaded groundnut shells and sawdust. In particular, the dye used in this study was the reactive orange 13. Authors found that there was an increment (up to 100%) of the metal adsorption capacities in these adsorbents at batch conditions. This increment in the adsorbent performance for metal removal is lower than that reported in the present study. Finally, it is convenient to remark that Thomas model was useful for modeling all breakthrough curves of both mono-component and binary solutions. It provided a good agreement between experimental and calculated dynamic adsorption data where R^2 ranged from 0.89 to 0.99.

3.3. Physico-chemical characterization of the activated carbon

Fig. 4 shows the FTIR spectra of selected samples of activated carbon with and without loaded pollutants using mono-component solutions. Overall, the spectra of both the raw and metal-loaded adsorbent (i.e. Fig. 4(a), (c) and (d)) are similar where the vibration bands are in the same position. The bands at 3,730 and 3,430 cm^{-1} correspond to the stretching vibration O–H of hydroxyl. The characteristic band of the stretching vibration C=C of aromatic compounds is located at ~1,700 cm^{-1}. The C=O band is identified at 1,616 cm^{-1} while the band of C–O stretching vibration is located at 1,180 cm^{-1} [16,31]. The vibrations of hydrogen in the aromatic compounds are found from 700 to 900 cm^{-1}. Finally, the absorption bands at 1,132 and 677 cm^{-1} indicate the presence of nitro groups on the carbon surface [32]. Fig. 4(b) shows that the adsorption of dye AB25 on the carbon surface increases the intensities of IR bands observed in the

Table 5
Design parameters of packed bed columns obtained from the breakthrough curves for the adsorption of heavy metal ions on dye-loaded activated carbon

		Design parameters of packed bed columns					Thomas model		
Pollutant	Feed concentration (mg/L)	t_b (h)	t_e (h)	Δt (h)	MTZ (cm)	r_f	K_{Th} (L/h mg)	q_{bed} (mg/g)	R^2
Ni^{2+}	20	21.85	69.8	47.95	5.15	1,140.29	0.1286	13.55	0.97
	30	18.0	71.66	53.66	5.62	862.74	0.0721	13.07	0.95
Zn^{2+}	20	33.63	66.25	32.62	3.69	1,605.46	0.0115	16.58	0.99
	30	20.21	56.26	36.05	4.81	1,212.66	0.0614	22.05	0.99

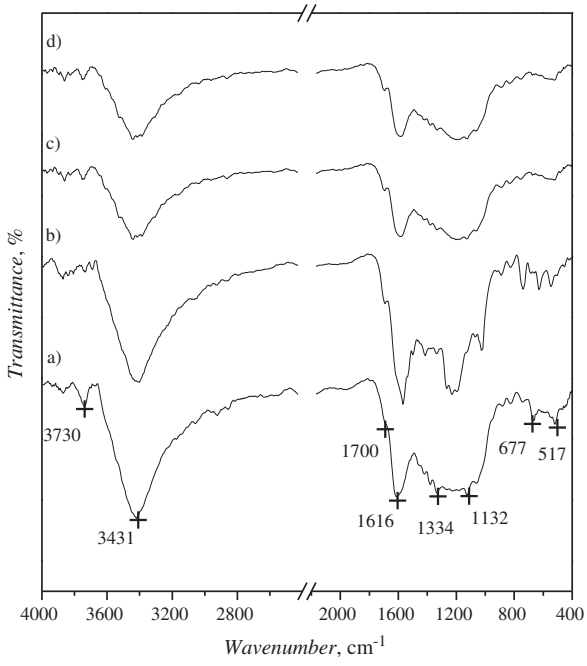

Fig. 4. FTIR spectra of activated carbon used in the adsorption of dye AB25, Ni^{2+} and Zn^{2+}. Sample: (a) raw activated carbon, (b) activated carbon loaded with dye AB25, (c) activated carbon after Zn^{2+} removal, and (d) activated carbon after Ni^{2+} removal.

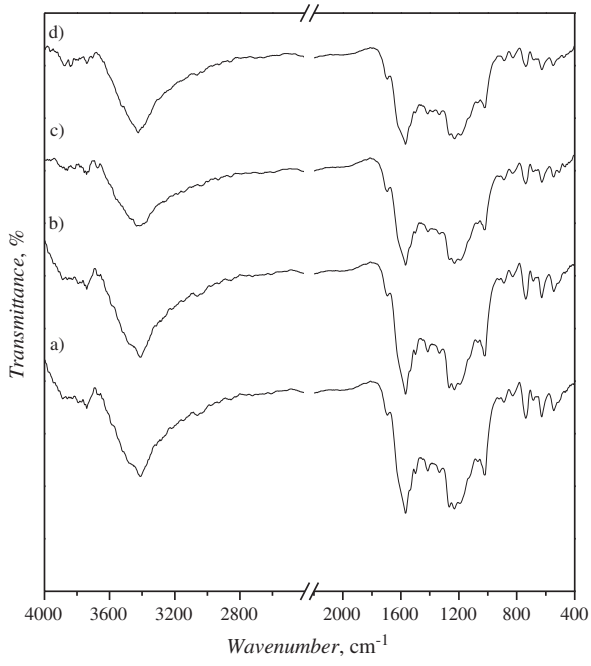

Fig. 5. FTIR spectra of (a) dye-loaded activated carbon after Zn^{2+} adsorption, (b) dye-loaded activated carbon after Ni^{2+} adsorption, (c) activated carbon after the simultaneous adsorption of dye AB25 and Zn^{2+}, and (d) activated carbon after the simultaneous adsorption of dye AB25 and Ni^{2+}.

range 1,700–517 cm^{-1}, which are associated to oxygenated functional groups. On the other hand, Fig. 5 shows the spectra of samples obtained from the experiments with the dye-loaded activated carbon that was used in the removal of heavy metals (Fig. 5(a) and (b)) and the raw adsorbent used in the simultaneous removal of heavy metal and dye (Fig. 5(c) and (d)). All these spectra show the same bands at identical positions but their intensities are different in the range 1,700–517 cm^{-1}. As stated, this region is characteristic of the functional groups of dye AB25 and the absorption bands identified for these samples correspond to those reported for Fig. 4.

XPS results are reported in Figs. 6–9. Specifically, the high resolution spectra of C 1s for selected samples are reported in Fig. 6. Note that the C 1s photoelectron peaks were also deconvoluted according to the binding energies of carbon bonds. Three Gaussians peaks are identified at binding energies of 284.6, 286.6, and 289.1 eV, which correspond to the following groups: C–C and C–H, C=O and O=C–O [33,34]. On the other hand, XPS spectra of O 1s are given in Fig. 7. Deconvolution of the O 1s band provided two sub-peaks around 531 and 533 eV, which are attributed to C=O and C–O bond type, respectively. It is convenient to remark that the activated carbon loaded with dye AB25 has the highest O 1s signal intensity, which is caused by the dye adsorption on the activated carbon surface that increases the presence of functional groups C=O. For illustration, the Zn 2p XPS spectra of the raw activated carbon and the dye-loaded activated carbon after Zn^{2+} removal are reported in Fig. 8. The Zn 2p spectrum does not exist in the sample of raw adsorbent; however, after Zn^{2+} adsorption on dye-loaded activated carbon, a new and unique peak is found. The energy band of this peak corresponds to 1,022 eV and, according to the data base, it can be associated to the bond Zn–O. This bond can be formed via the displacement of the Na^{+} ions by Zn^{2+} ions in the auxochrome functional group $NaSO_3$ of the dye molecule loaded on the surface of activated carbon. Finally, Fig. 9 shows the S 2p spectra for the same samples analyzed in Fig. 8. Results indicated that the signal increases considerably for samples obtained from dye removal due to the incorporation of the group S=O and S–O–Na of the dye molecule loaded on the surface of activated carbon. Note that this peak decreased in the sample of dye-loaded activated carbon used for Zn^{2+} removal, which suggests the formation of the bond S–O–Zn. Similar findings have been obtained for adsorbent samples used in Ni^{2+} removal. In summary, it is clear that surface

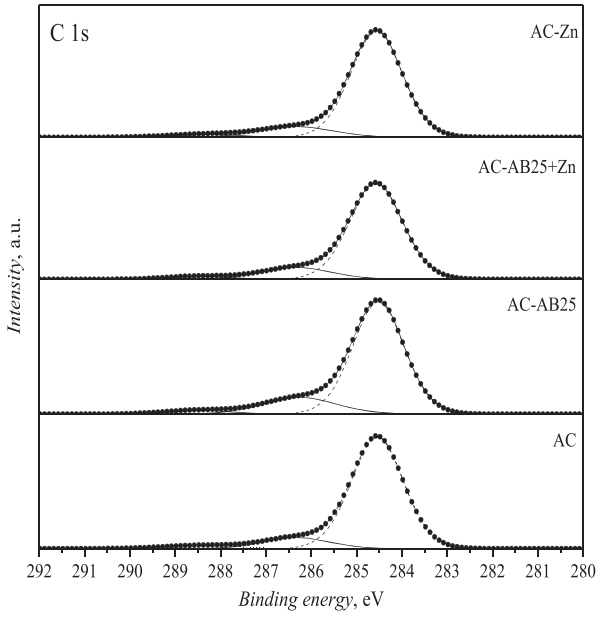

Fig. 6. High resolution C 1s photoelectron spectra of activated carbon samples used in dynamic adsorption experiments. Samples: raw activated carbon (AC), dye-loaded activated carbon (AC–AB25), dye-loaded activated carbon after Zn^{2+} removal (AC–AB25 + Zn), and activated carbon after Zn^{2+} removal (AC–Zn).

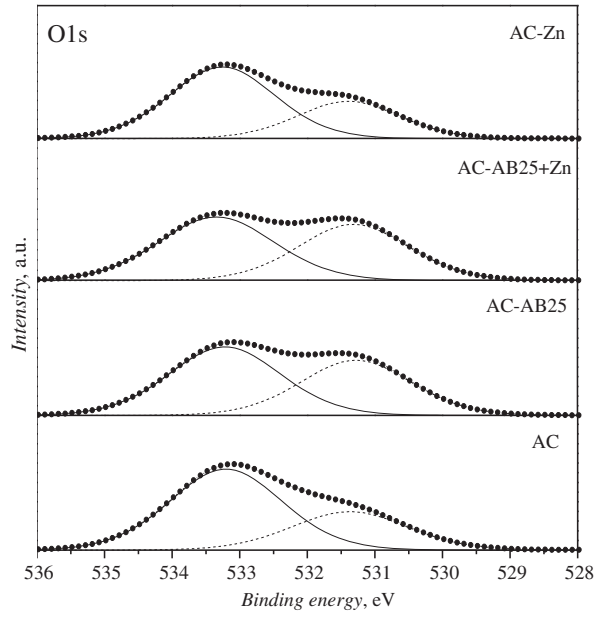

Fig. 7. High resolution O 1s photoelectron spectra of activated carbon samples used in dynamic adsorption experiments. Samples: raw activated carbon (AC), dye-loaded activated carbon (AC-AB25), dye-loaded activated carbon after Zn^{2+} removal (AC–AB25 + Zn), and activated carbon after Zn^{2+} removal (AC–Zn).

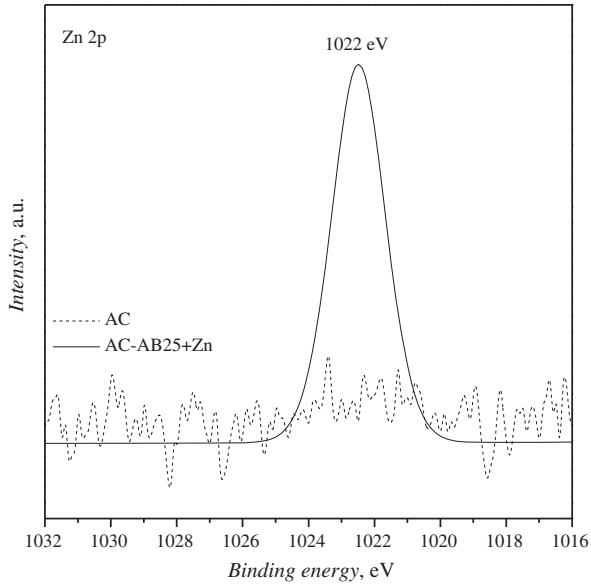

Fig. 8. XPS Zn 2p spectra of activated carbon samples used in dynamic adsorption experiments. Samples: raw activated carbon (AC) and dye-loaded activated carbon after Zn^{2+} removal (AC–AB25 + Zn).

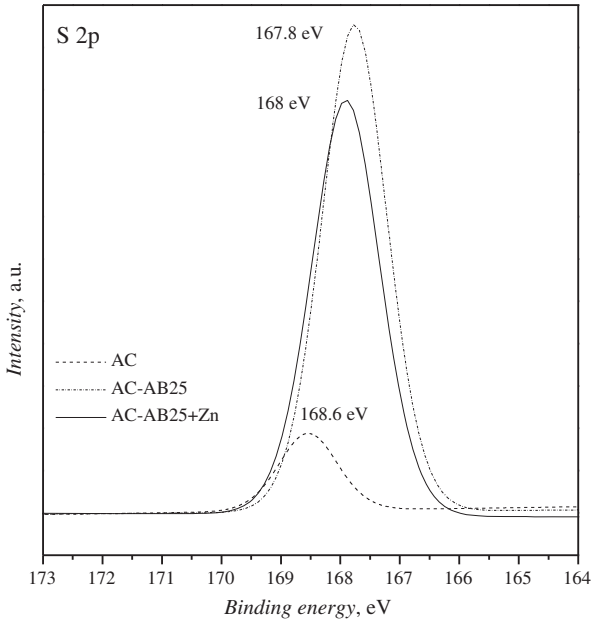

Fig. 9. XPS S 2p spectra of activated carbon samples used in dynamic adsorption experiments. Samples: raw activated carbon (AC), dye-loaded activated carbon (AC–AB25), and dye-loaded activated carbon after Zn^{2+} removal (AC–AB25 + Zn).

reactions exist between metallic ions and S=O functional groups of dye-loaded activated carbon.

Results of this study are useful for understanding the role of dye AB25 in the synergistic adsorption of

both Ni^{2+} and Zn^{2+} ions in binary systems. In fact, this synergistic adsorption effect is due to the AB25 adsorbed on the surface of activated carbon acts as an active site for the adsorption of metallic ions. Therefore, this adsorption mechanism is relevant for the simultaneous adsorption of both dye AB25 and heavy metal ions in binary systems in both dynamic and batch operating conditions.

4. Conclusions

This study reports the simultaneous adsorption of AB25, Ni^{2+} and Zn^{2+} in binary mixtures of dye and metal using packed bed adsorption columns with activated carbon. Design parameters have been calculated for the breakthrough curves obtained from binary solutions and a comparative has been performed with the results obtained with mono-component solutions and with experiments performed using dye-loaded activated carbon. This study showed that there is a strong synergistic adsorption of heavy metals on activated carbon caused by the presence of dye AB25 in binary mixtures of dye and metal under dynamic operating conditions. The magnitude of this synergistic adsorption effect depends on the dynamic operating conditions and type of heavy metal present in the binary system. In fact, the presence of dye AB25 in the binary mixtures caused a better degree of column utilization due to the values of MTZ decreased with respect to the results obtained with mono-component solutions. Metal adsorption capacities may increase up to 20 times if the binary mixture with dye AB25 is used as a column feed. In addition, the removal of heavy metal ions in adsorption columns packed with dye-loaded activated carbon is also an effective treatment process. This improvement in metal adsorption capacities is due to dye AB25 loaded in activated carbon may act as an additional active site for binding metallic ions. Results showed that an adsorbent with a lower adsorption capacity for the removal of heavy metals can be employed, without comprising the process efficacy, in the treatment of multicomponent mixtures of dyes and heavy metals under dynamic operating conditions. In summary, this study reports new insights about the performance of activated carbon for the adsorption of water pollutants in multicomponent systems using packed bed columns.

References

[1] T. Bohli, A. Ouederni, N. Fiol, I. Villaescusa, Single and binary adsorption of some heavy metals ions from aqueous solutions by activated carbon derived from olive stones, Desalin. Water Treat. 53 (2013) 1082–1088.

[2] D. Nabarlatz, J. de Celis, P. Bonelli, A.L. Cukierman, Batch and dynamic sorption of Ni(II) ions by activated carbon based on a native lignocellulosic precursor, J. Environ. Manage. 97 (2012) 109–115.

[3] H. Treviño-Cordero, L.G. Juárez-Aguilar, D.I. Mendoza-Castillo, V. Hernández-Montoya, A. Bonilla-Petriciolet, M.A. Montes-Morán, Synthesis and adsorption properties of activated carbons from biomass of *Prunus domestica* and *Jacaranda mimosifolia* for the removal of heavy metals and dyes from water, Ind. Crops. Prod. 42 (2013) 315–323.

[4] D. Mohan, S. Chander, Single component and multi-component adsorption of metal ions by activated carbons, Colloids Surf., A 177 (2001) 183–196.

[5] H.E. Reynel-Avila, D.I. Mendoza-Castillo, V. Hernández-Montoya, A. Bonilla-Petriciolet, Multicomponent removal of heavy metals from aqueous solution using low-cost sorbents, in: B. Antizar-Ladislao, R. Sheikholeslami (Eds.), Water Production and Wastewaters Treatment, Editorial Nova Science Publisher, New York, 2011, pp. 69–99.

[6] C. Escudero, J. Poch, I. Villaescusa, Modelling of breakthrough curves of single and binary mixtures of Cu(II), Cd(II), Ni(II) and Pb(II) sorption onto grape stalks waste, Chem. Eng. J. 217 (2013) 129–138.

[7] K.Y. Foo, B.H. Hameed, An overview of dye removal via activated carbon adsorption process, Desalin. Water Treat. 19 (2010) 255–274.

[8] J. Lach, E. Okoniewska, L. Stępniak, A. Ociepa-Kubicka, The influence of modification of activated carbon on adsorption of Ni(II) and Cd(II), Desalin. Water Treat. 52 (2014) 3979–3986.

[9] J.M. Dias, M.C.M. Alvim-Ferraz, M.F. Almeida, J. Rivera-Utrilla, M. Sánchez-Polo, Waste materials for activated carbon preparation and its use in aqueous-phase treatment: A review, J. Environ. Manage. 85 (2007) 833–846.

[10] F. Fu, Q. Wang, Removal of heavy metal ions from wastewaters: A review, J. Environ. Manage. 92 (2011) 407–418.

[11] M.A.M. Salleh, D.K. Mahmoud, W.A.W.A. Karim, A. Idris, Cationic and anionic dye adsorption by agricultural solid wastes: A comprehensive review, Desalination 280 (2011) 1–13.

[12] G. Mezohegyi, F.P. van der Zee, J. Font, A. Fortuny, A. Fabregat, Towards advanced aqueous dye removal processes: A short review on the versatile role of activated carbon, J. Environ. Manage. 102 (2012) 148–164.

[13] M.T. Yagub, T.K. Sen, S. Afroze, H.M. Ang, Dye and its removal from aqueous solution by adsorption: A review, Adv. Colloid Interface 209 (2014) 172–184.

[14] M. Visa, C. Bogatu, A. Duta, Simultaneous adsorption of dyes and heavy metals from multicomponent solutions using fly ash, Appl. Surf. Sci. 256 (2010) 5486–5491.

[15] X. Li, Y. Li, S. Zhang, Z. Ye, Preparation and characterization of new foam adsorbents of poly(vinyl alcohol)/chitosan composites and their removal for dye and heavy metal from aqueous solution, Chem. Eng. J. 183 (2012) 88–97.

[16] R. Tovar-Gómez, D. Rivera-Ramírez, V. Hernández-Montoya, A. Bonilla-Petriciolet, C. Durán-Valle, M.A. Montes-Morán, Synergic adsorption in the simultaneous removal of acid blue 25 and heavy metals from

water using a Ca(PO3)2-modified carbon, J. Hazard. Mater. 199–200 (2012) 290–300.
[17] I.A. Aguayo-Villarreal, V. Hernández-Montoya, A. Bonilla-Petriciolet, R. Tovar-Gómez, E.M. Ramírez-López, M.A. Montes-Morán, Role of acid blue 25 dye as active site for the adsorption of Cd2+ and Zn2+ using activated carbons, Dyes Pigm. 96 (2013) 459–466.
[18] J.H. Deng, X.R. Zhang, G.M. Zeng, J.L. Gong, Q.Y. Niu, J. Liang, Simultaneous removal of Cd(II) and ionic dyes from aqueous solution using magnetic graphene oxide nanocomposite as an adsorbent, Chem. Eng. J. 226 (2013) 189–200.
[19] V. Hernández-Montoya, M.A. Pérez-Cruz, D.I. Mendoza-Castillo, M.R. Moreno-Virgen, A. Bonilla-Petriciolet, Competitive adsorption of dyes and heavy metals on zeolitic structures, J. Environ. Manage. 116 (2013) 213–221.
[20] N.P. Jović-Jovičić, A.D. Milutinović-Nikolić, M.J. Žunić, Z.D. Mojović, P.T. Banković, I.A. Gržetić, D.M. Jovanović, Synergic adsorption of Pb^{2+} and reactive dye—RB5 on two series of organomodified bentonites, J. Contam. Hydrol. 150 (2013) 1–11.
[21] G.Z. Kyzas, N.K. Lazaridis, M. Kostoglou, On the simultaneous adsorption of a reactive dye and hexavalent chromium from aqueous solutions onto grafted chitosan, J. Colloid Interface Sci. 407 (2013) 432–441.
[22] J.P. Chen, X. Wang, Removing copper, zinc and lead ion by granular activated carbon in pretreated fixed-bed columns, Sep. Purif. Technol. 19 (2000) 157–167.
[23] C.Y. Yin, M.K. Aroua, W.M.A.W. Daud, Fixed-bed adsorption of metal ions from aqueous solution on polyethyleneimine-impregnated palm shell activated carbon, Chem. Eng. J. 148 (2009) 8–14.
[24] R. Tovar-Gómez, M.R. Moreno-Virgen, J.A. Dena-Aguilar, V. Hernández-Montoya, A. Bonilla-Petriciolet, M.A. Montes-Morán, Modeling of fixed-bed adsorption of fluoride on bone char using a hybrid neural network approach, Chem. Eng. J. 228 (2013) 1098–1109.
[25] I.A. Aguayo-Villarreal, A. Bonilla-Petriciolet, V. Hernández-Montoya, M.A. Montes-Morán, H.E. Reynel-Avila, Batch and column studies of Zn^{2+} removal from aqueous solution using chicken feathers as sorbents, Chem. Eng. J. 167 (2011) 67–76.
[26] R. Apiratikul, P. Pavasant, Batch and column studies of biosorption of heavy metals by *Caulerpa lentillifera*, Bioresour. Technol. 99 (2008) 2766–2777.
[27] H.C. Thomas, Heterogeneous ion exchange in a flowing system, J. Am. Chem. Soc. 66 (1944) 1664–1666.
[28] A. Bonilla-Petriciolet, M.G. Lira-Padilla, C.A. Soto-Becerra, Aplicación del método de optimización de recocido simulado en la regresión de isotermas de adsorción (Application of the simulated annealing optimization method for the fitting of adsorption isotherms), Rev. Int. Contaminación Ambiental 21 (2005) 201–206.
[29] H. Kalavathy, B. Karthik, L.R. Miranda, Removal and recovery of Ni and Zn from aqueous solution using activated carbon from *Hevea brasiliensis*: Batch and column studies, Colloids Surf., B 78 (2010) 291–302.
[30] S.R. Shukla, R.S. Pai, Adsorption of Cu(II), Ni(II) and Zn(II) on dye loaded groundnut shells and sawdust, Sep. Purif. Technol. 43 (2005) 1–8.
[31] C.J. Durán-Valle, M. Gómez-Corzo, J. Pastor-Villegas, Study of cherry stones as raw material in preparation of carbonaceous adsorbents, J. Anal. Appl. Pyrol. 73 (2005) 59–67.
[32] A.E. Ghali, M. Baouab, M.S. Roudesli, M.S. Roudesli, Preparation, characterization and application of a [copper (II)/ethylenediamine–cotton] complex for the removal of AB25 from aqueous solution in a laboratory scale column, Chem. Eng. J. 174 (2011) 18–26.
[33] A. Rudrake, K. Karan, J.H. Horton, A combined QCM and XPS investigation of asphaltene adsorption on metal surfaces, J. Colloid Interface Sci. 332 (2009) 22–31.
[34] M.H. Ahmed, J.A. Byrne, J.A.D. McLaughlin, A. Elhissi, W. Ahmed, Comparison between FTIR and XPS characterization of amino acid glycine adsorption onto diamond-like carbon (DLC) and silicon doped DLC, Appl. Surf. Sci. 273 (2013) 507–514.